EXPERIMENTAL INVESTIGATION OF AERODYNAMIC FORCES AND SHOCK WAVES FOR A WAVERIDER IN SUPERSONIC AND SLIP REGIME CARRIED OUT IN THE MARHY FACILITY

Viviana Lago, Noubel Hugo

EXPERIMENTAL INVESTIGATION OF AERODYNAMIC FORCES AND SHOCK WAVES FOR A WAVERIDER IN SUPERSONIC AND SLIP REGIME CARRIED OUT IN THE MARHY FACILITY

A. Hugo Noubel, B. Viviana Lago,

CNRS, ICARE, UPR 3021, 1c av. de la Recherche Scientifique, Orléans cedex 2, France A-B

ABSTRACT

Hypersonic vehicles are more and more studied in the military domain but also for other missions as the interplanetary or commercial missions. These vehicles optimize the ratio between lift and drag forces to success their missions. Hypersonic vehicles studied are launched at high altitude by rockets and they realize a re-entry by changing their angle of attack in function of speed and altitude. In this study, aerodynamic forces (drag and lift) are experimentally measured for different angles of attack and for four different rarefied flows conditions representative of altitudes ranging between 50 km and 80 km. The first part focus on aerodynamic forces and the behavior of the vehicle at altitudes higher than the initial optimal one which is 50 km in this case. The second part consists to study the shock angles at same angles of attack and rarefied flows to correlate shock wave angles and aerodynamic forces.

Index Terms— Waverider, Wind tunnel, Supersonic rarefied flow, Lift-to-Drag ratio, Shock wave

1. INTRODUCTION

Hypersonic flight is increasingly sought after worldwide for a variety of missions. The design of hypersonic vehicles change according the mission but the common requirement for all missions is to obtain the greatest Lift-to-Drag ratio. The higher this parameter is, the longer the waverider will travel. Hypersonic vehicles could be used for different missions: military [1], interplanetary [2] or commercial [3]. They are two types of hypersonic vehicles: the Hypersonic Cruise Missiles (HCM) as the X-51A waverider and the Hypersonic Glide Vehicles (HGV) as the HTV-2 [4] which has no propulsion. In this study, only hypersonic glide vehicles will be considered. Several countries have already developed their own vehicles, such as United States with the HTV-2, China with the DF-ZF [1] or Russia with the Avangard [5].

Hypersonic gliders do not have booster and they are launched by rockets at high altitude (between 50 km and 100 km). For this type of vehicle, the re-entry trajectory is important and constitutes a real challenge. In his article, Linshu [6] presents a schematic trajectory with the different phases of the re-entry into the atmosphere. The trajectory and capabilities of hypersonic vehicles give them unprecedented attributes and an ability to be unpredictable. Trajectory design performance is the essential section of a spacecraft [7]. All trajectory optimization strategies [8] are based on an inviscid flow field [9].

However, part of the waverider trajectory takes place at high altitude and the assumption of an inviscid flow is not relevant. To design a waverider, one of the methods used is the Rasmussen method [10] which considers only the inviscid flow. This method is relevant for low altitudes but a realistic method must consider: viscous effects with wall shear stress, weak and strong hypersonic viscous interaction, boundary layer displacement and the effects of sliding flow at high altitudes. [11]. Low density effects affect and significantly reduce the Lift-to-Drag ratio [12]. To improve the performance of waveriders in the low-density regime, Anderson, Bowcut, and Corda proposed a new method of geometry design in 1986 [13, 14]. This method involves introducing skin friction into the geometry optimization process. This change introduces the new family of waveriders called optimized viscous hypersonic waveriders.

In the upper atmosphere and low density, the assumption of a continuous flow regime fails. Depending on the Mach number and the density of the flow, the flow regime can be considered as a slip flow or a transitional flow [15]. In these regimes, to describe the interaction between the molecules, statistical methods are required such as the Boltzman equation. To solve this equation, the most appropriate numerical simulation is the direct Monte Carlo simulation (DSMC) proposed by Prof. Bird. Many numerical simulations have been performed to identify rarefaction effects [16, 17]. To complete and validate the numerical simulations, experimental data are needed. A few studies have been performed in rarefied domain with delta wings [18, 19]. The few experiments are due to a lack of facilities and the main researches on the waverider in wind tunnel were realized at medium altitude: 22.5 km for Nagashetty [20], 30.6 km for Rolim [21]. Cockrell [22] performed aerodynamic force measurements in a Mach 4 flow with a waverider at a Reynolds number equal to 3.99×10^{-6}. Only a few numerical studies have been performed in the rarefied regime [23, 24]. Most of the work on the waverider topic focuses on the study the aerody-

namic forces in order to optimize the geometries and improve the Lift-to-Drag ratio. Regarding the study of waverider impact angles, there are few studies. Anderson [25] presents a method for determining the variation of the thickness of a normal shock as a function of Mach number and altitude. The method is based on the Grad steady state to obtain the thickness of the normal shock and the method is confirmed in 1955 by Shermann. In 1979 Allegre proposed in his thesis [26] experimental data on the shock angles of delta wings in rarefied regime.

The main objective of this work is to experimentally study the aerodynamic forces and shock angles of a waverider in several slip regime flows at different Knudsen number. The chosen waverider is based on Rolim's waverider [21] which was designed with the Rasmussen method for Mach 10 - 50 km. In a first step, the objective is to analyze the behavior of the vehicle in off-design flow conditions and to evaluate the degradation of the Lift-to-Drag ratio for different velocities and pressures typical to altitudes ranged between 50 km and 80 km. The shock wave angles are analyzed to characterise the evolution of the upper and lower shocks angles. General equations are proposed to describe shock waves of both sides of the model as a function of Mach number and free stream density for any angle of attack. Finally, a discussion is proposed to correlate the aerodynamic forces and shock wave angles, including viscous layers.

2. EXPERIMENTAL CONDITION

2.1. Waverider model

The geometry of waverider investigated is based on the geometry of the Rolim waverider which contributed to the development of the Brazilian waverider named 14-X. The model of the vehicle was built with the Rasmussen method. The optimal flight conditions for this waverider are a Mach number of 10 and an altitude ranged between 40 km and 50 km. In the present study, experiments were carried out with flows at Mach numbers 2 and 4 and free stream pressure flows ranged between 2.67 Pa and 71 Pa which corresponds to a range of altitudes between 60 km and 80 km. The objective is to study the aerodynamic behavior of the waverider in off-design conditions. In this study, the waverider is confronted with slip regime and flows more viscous than those with pressures representative of the 50 km altitude.

The Rolim waverider has been scaled to match with the flow core size of the experimental conditions the MARHy wind tunnel. The test model is therefore 100 mm long, 35.7 mm wide and 6.6 mm high. The non-dimensional parameters used in this paper were determined with a characteristic of 100 mm. The top surface is slightly curved.

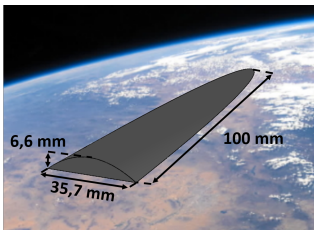

Fig. 1: Waverider geometry

2.2. Wind tunnel description

The MARHy (Mach Adaptable Rarefied Hypersonic) wind tunnel can recreate supersonic and hypersonic flows at low density to simulate the rarefied flows conditions at high atmospheric altitude.

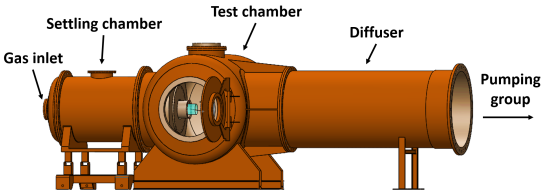

Fig. 2: Wind tunnel MARHy

The facility can be divided in two parts: the wind tunnel and the pumping unit. The wind tunnel consists of three elements.

In the flow direction, the first element is the settling chamber, then there is the nozzle and finally the experimental chamber. In supersonic configuration, the settling chamber is a tank where the gas (air) is introduced before passing through the nozzle. The pressure is controlled by a micrometric valve to obtain the stagnation pressure P_0 of the used nozzle. All conditions in the settling chamber are considered to be stagnation conditions and are indicated by the index 0 (in Table 1, Table 2, Table 3 and Table 4). The second element of the test chamber is the nozzle. In supersonic conditions contoured and a set of different nozzles are availed to create a flow with a single Mach number and a single free flow pressure. For this study, four flow conditions were studied with four different nozzles to be changed for each new experimental condition. The last element is the test chamber where the test model is located. It is connected with the pumping unit by the diffuser.

The pumping unit consists of two primary pumps, two intermediate roots pumps, and twelve high vacuum roots pumps. The operating conditions of the profiled nozzle determine the number of pumps needed to stabilize the correct static pressure inside the test chamber. The free stream pressure P_∞ is adjusted operating the motorized butterfly valve

placed between the wind tunnel and the pumping group. The pumping unit allows for unlimited test time unlike other wind tunnels.

2.3. Operating conditions

Each experimental condition in supersonic rarefied configurations requires a specific profiled nozzle. In this study, four supersonic flows are studied and the associated nozzles are presented in this section. The nozzles were chosen to study the impact of Mach number variation and static pressure variation on aerodynamic forces and shock waves. Three nozzles are dedicated to the study of the impact of the pressure: Mach 4 - 2.67 Pa, Mach 4 - 8 Pa and Mach 4 - 71 Pa. The Mach 4 - 8 Pa nozzle is also used to study the impact of the Mach number with the Mach 2 - 8 Pa nozzle. Force measurements with aerodynamic balance were carried out in all the experimental conditions. Regarding flow visualization and shock waves analysis, the experimental condition at P_∞ = 71.11 Pa could not be investigated because the glow discharge technique cannot be applied.

Table 1: Flow conditions of the Mach 2 - 8 Pa nozzle

Stagnation conditions		**Free-stream conditions**	
gas	ambient air	gas	ambient air
P_o (Pa)	62.58	P_∞ (Pa)	8
Te_o (K)	293	Te_∞ (K)	162.78
ρ_o (kg.m^{-3})	7.44×10^{-4}	ρ_∞ (kg.m^{-3})	1.71×10^{-4}
		μ_∞ (Pa.s)	1.11×10^{-5}
		U_∞ (m.s^{-1})	511.43
		Re_∞ (m^{-1})	7738.6
		Ma_∞	2.0
		λ_∞ (m)	2.79×10^{-4}

Table 2: Flow conditions of the Mach 4 - 2.67 Pa nozzle

Stagnation conditions		**Free-stream conditions**	
gas	ambient air	gas	ambient air
P_o (Pa)	404.79	P_∞ (Pa)	2.67
Te_o (K)	293	Te_∞ (K)	69.76
ρ_o (kg.m^{-3})	4.82×10^{-3}	ρ_∞ (kg.m^{-3})	1.33×10^{-4}
		μ_∞ (Pa.s)	4.78×10^{-6}
		U_∞ (m.s^{-1})	669.61
		Re_∞ (m^{-1})	18 049
		Ma_∞	4.0
		λ_∞ (m)	2.20×10^{-4}

3. EXPERIMENTS DESCRIPTION

3.1. Aerodynamic sting balance

A home-made aerodynamic balance has been developed and used to measure forces in supersonic and hypersonic rarefied flows. It is a two-axis balance that measures drag and lift forces applied to the model.

Table 3: Flow conditions of the Mach 4 - 8 Pa nozzle

Stagnation conditions		**Free-stream conditions**	
gas	ambient air	gas	ambient air
P_o (Pa)	1214.39	P_∞ (Pa)	8
Te_o (K)	293	Te_∞ (K)	69.76
ρ_o (kg.m^{-3})	1.44×10^{-2}	ρ_∞ (kg.m^{-3})	4.00×10^{-4}
		μ_∞ (Pa.s)	4.78×10^{-6}
		U_∞ (m.s^{-1})	669.61
		Re_∞ (m^{-1})	54 147
		Ma_∞	4.0
		λ_∞ (m)	7.33×10^{-5}

Table 4: Flow conditions of the Mach 4 - 71 Pa nozzle

Stagnation conditions		**Free-stream conditions**	
gas	ambient air	gas	ambient air
P_o (Pa)	10797.3	P_∞ (Pa)	71.11
Te_o (K)	293	Te_∞ (K)	69.76
ρ_o (kg.m^{-3})	1.28×10^{-1}	ρ_∞ (kg.m^{-3})	3.55×10^{-3}
		μ_∞ (Pa.s)	4.78×10^{-6}
		U_∞ (m.s^{-1})	669.61
		Re_∞ (m^{-1})	497 800
		Ma_∞	4.0
		λ_∞ (m)	1.2×10^{-5}

The balance is composed of two modules that separately measure the two forces. Each module is designed with thin strips that are perpendicular to the force they measure. Strain gauges are attached to the strips and characterize the deformation by a variation of the electrical signal. Then, a calibration with a digital Newtonmeter allows to correlate the variation of the signal and the force.

Different angles of attack are studied. To measure the forces for each angle, the sting balance is positioned horizontally on a rotating device and thus avoid gravity forces. Otherwise, The drag depends on the position of the center of gravity, so a change in the center of gravity may induce a new calibration. After each rotation, the test model and balance are moved by a motorized robot to maintain the same flow conditions around the test model.

To measure the drag and lift forces, the waverider is positioned in the flow and an initial ten seconds recording is made. During this recording, one thousand points are recorded every second. Next, the parasite forces that can act on the balance are measured. To do this, a flat plate is placed in front of the model so that the flow no longer interacts with the waverider. A new recording of ten seconds is made. This second recording allows to characterize the parasite forces and particularly the one created by the pumping group. The forces due to the flow acting on the waverider are the result of the difference between the two sets of recordings.

This experimental protocol is realized five times for each angle of attack to improve the accuracy of measurements. Drag and lift forces depend on the angle of attack values so trigonometric formulas are used to correct forces and decorrelate the drag and lift [27]. The standard deviation was determined for all four nozzles and on average the drag force has a standart deviation of 1.86 mN and 0.6 mN for the lift module. All details are represented by error bars on each value of each graphs (Figure 3, Figure 4, Figure 5 and Figure 6).

3.2. Glow discharge

To observe waverider shock waves in rarefied flows, only the glow discharge method is possible. For moderate pressures, as is the case for the Mach 4 - 71 Pa nozzle, the glow discharge technique does not allow the flow to be visualized because the discharge remains confined around the electrode due to the pressure.

The glow discharge technique consists of weakly ionising the gas using a negatively polarized copper ring which is placed at the outlet of the nozzle. The ionization creates a pink glow. Ionization produces excited molecules of N_2 and N_2^+ emitting photons at wavelengths 337 nm for the positive system 2^{nd} and 391.4 for the negative system 1^{st} [28].

Ionized flow field around the model is captured with the ICCD Kuro camera. For each angle of attack, three different images are recorded with different exposure times. To improve the quality of the images, the background flow field without the model is recorded to have a better contrast on the shock wave. The shock wave is then highlighted and can be detected with the software ImageJ. The analysis of the shock waves shows that near the nose, the shock shape is rounded because the thick boundary layer is merged. The angle of the shock wave have been determined from the middle axis of the test model to the end because the shape can be approximated by a linear evolution . This method gives angles values with an accuracy ranging from 0.048 degrees to 2.59 degrees. When applying an angle of attack to the waverider, the lower shock will become more visible, with a low accuracy of the shock wave angle value, and the presicion on this detection will be better which is the opposite with the upper angle.

4. RESULTS

4.1. Lift, drag forces and Lift-to-Drag ratio

For hypersonic glide booster vehicles, the most important parameter during flight is the Lift-to-Drag ratio. These vehicles have no boosters, so they must optimize their angle of attack and Lift-to-Drag ratio to glide the greatest distance possible. The Lift-to-Drag ratio is the ratio of horizontal distance traveled for each unit of vertical distance lost. For example, a ratio of two means that the waverider glides two kilometers horizontally for every vertical kilometer lost. The goal of waveriders is to decrease drag and increase lift to maximize the ratio of both.

For each experimental condition, the angles of attack investigated range between 0 degree and 25 degrees. For these angles, the waverider has its nose higher than its base like an airplane during take-off. The objective of these experiments is to visualize the evolution of the drag force, the lift force and the Lift-to-Drag ratio as a function of the angle of attack, the Mach number and the free stream pressure. These two last parameters will define the rarefaction parameter. Nevertheless, giving an angle of attack to the wave rider, le local flow on the upper and lower side of the waverider will be different leading to different local rarefaction parameter. Figure 3, Figure 4, Figure 5 and Figure 6 show the evolution of the two aerodynamic forces as a function of the angle of attack. The trend of the two forces is different but similar for all experimental conditions. The drag describes a parabolic curve which has a minimum near 0 degree. At this angle, the waverider has the better aerodynamic behavior because its wet section is the smallest of all configurations (angles of attack)follows. It is an advantage to have the lowest drag but it is the worst case if we consider the lift curve. Indeed, the lift curve describes a straight line as a linear function. In aerodynamics, the lift of lifting bodies has a maximum which is synonymous with stall. Thus, the angle of attack range describes only one part of the total lift curve. The maximum angle of attack studied is 25 degree because beyond the waverider blocks the central flow. Force measured at Mach 4 - 2.67 Pa and Mach 2 - 8 Pa are the lowest because flows they are the most rarefied, with the lowest density.

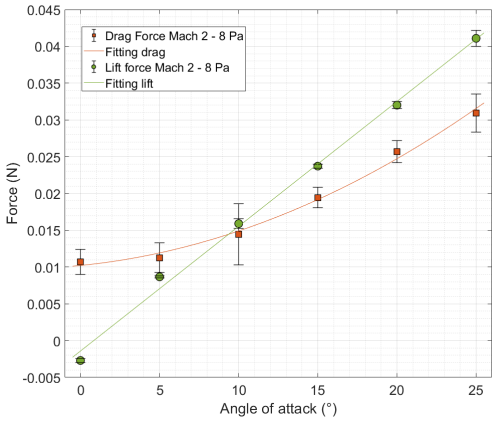

Fig. 3: Drag and lift at Mach 2 - 8 Pascals

The optimal angle of attack for the waverider is the angle for which the ratio of lift to drag is maximum. At this point, the waverider can travel the maximum distance. The goal during cruise is to maintain the highest possible Lift-to-Drag ratio to be sure to reach the landing point.

Figure 7 shows that the maximum Lift-to-Drag ratio is not

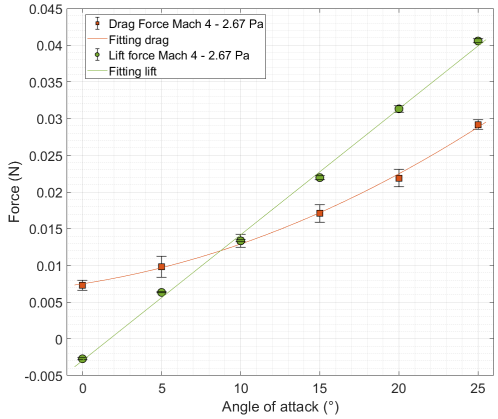

Fig. 4: Drag and lift at Mach 4 - 2 Pascals

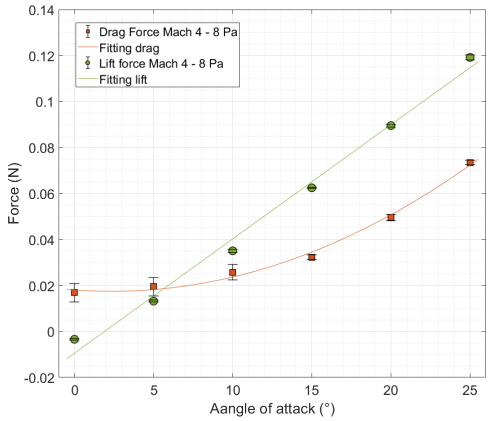

Fig. 5: Drag and lift at Mach 4 - 8 Pascals

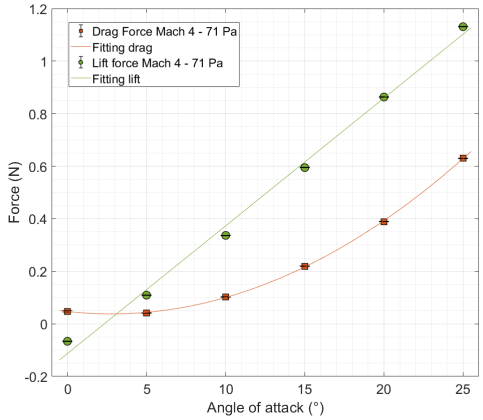

Fig. 6: Drag and lift at Mach 4 - 71 Pascals

reached for the same angle of attack for all the experimental conditions. However, the maximum of the values is different and the highest Lift-to-Drag ratio is reached for Mach 4 - 71 Pa at 10 degrees angle of attack. This flow condition is the least rarefied and represents the lowest altitude (50 km) in terms of viscous effects. Thus, in correlation with the altitudes, nozzle for which flow conditions have the greatest viscous parameter is the Mach 2 - 8 Pa and for which the maximum value of Lift-to-Drag ratio is the lowest . Thus, during a re-entry, the Lift-to-Drag ratio will increase and the angle of attack corresponding to the maximum value will decrease when the altitude decreases (decrease of the rarefaction degree). The angle of attack has an impact on aerodynamic performances and it is important to change it during the flight to keep the best trajectory possible.

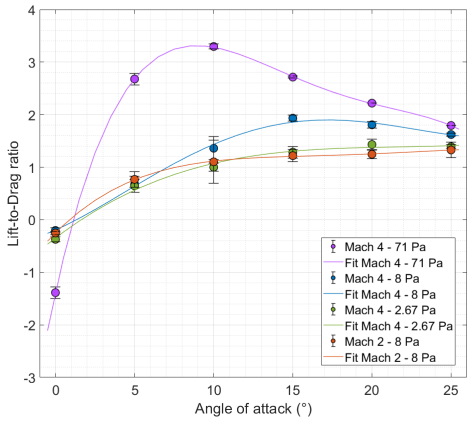

Fig. 7: Lift-to-Drag ratio curves of all flows conditions

Regarding flow conditions at Mach number 4, we observed that the increase in pressure is synonymous with an increase in the Lift-to-Drag ratio. The variation of pressure has a great impact on aerodynamic performances and the waverider is more operational in low altitude. But during a re-entry into the atmosphere, the waverider does not keep the same speed. If we analyze the two nozzles at 8 pascals, we can conclude that the increase in speed increases the performance of the waverider.

In conclusion, the Lift-to-Drag ratio increases when the altitude decreases and the speed increases. Thus if this waverider is launched from the rocket at 80 km of altitude, its aerodynamic performances will be weak (low Lift-to-Drag ratio). During the first phase of the re-entry (80 km to 50 km) the speed and the pressure will increase as waverider trajectories predict it [7] and the waverider will begin to improve its performances and will glide. The L/D maximum value will be reached at 50 km for a Mach number of 10 are the flight conditions for which the design has been optimised. The study shows that when a waverider is optimized for a low or medium altitude, it will have a difficult first re-entry phase. The waverider is not adapted to the rarefied domain and it can be improved by taking into account the boundary

layer in the optimization part as proposed by Anderson [12]. This can improve the maximum flight range.

4.2. Shock wave angle study

A waverider geometry is designed with the shock wave obtained by a supersonic or hypersonic flow over a cone in inviscid flows . The purpose is to analyze the shock wave angles of the waverider to see if a correlation with aerodynamic forces is possible. if so, it could help to optimise the geometry of the waverider.

The Mach 2 - 8 Pa, Mach 4 - 2.67 Pa and Mach 4 - 8 Pa flows are studied with the glow discharge method. Different angles of attack are studied: 0 degree to 25 degrees, same angles as the aerodynamic forces to compare both results.

The shock wave angle is divided into two regions: the upper shock angle and the lower shock angle. The variation of the upper shock angle is presented in Figure 8 and that of the lower shock in Figure 9.

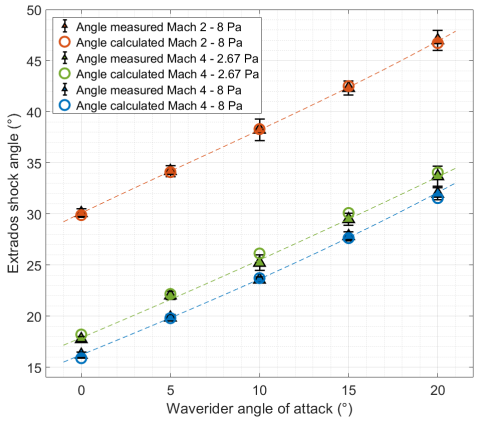

Fig. 8: Upper shock

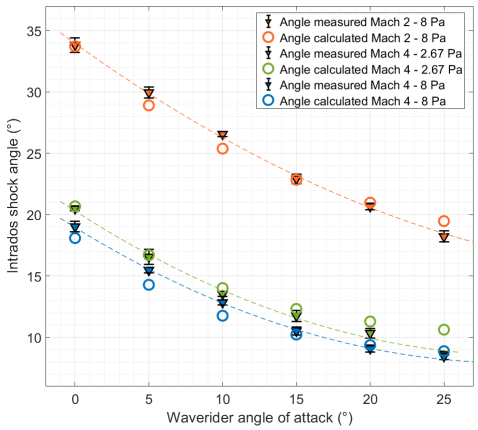

Fig. 9: Lower shock

On the upper shock angle Figure 8, the general trend is similar for all experimental conditions presenting a linear behavior that shows an opening of the shock angle as the angle of attack increases. The increase in the shock angle is well known in the continuous regime with the work of Anderson [29] but in the rarefied regime the phenomenon is amplified because of the thickening of the boundary layer. Accuracy decreases as the flow become more viscous and shock waves more diffuse, thus the error bar increases with the angle of attack, which is typical of a diffuse shock. The shock is difficult to be precisely detected and the accuracy decreases.

On the other hand, Figure 9, the shock angle decreases and approaches the waverider surface as the angle of attack increases. This trend is the same for any flow condition. A convergence appears when the angle of attack is higher than 20 degrees.

The most rarefied nozzle is Mach 2 - 8 Pa, then Mach 4 - 2.67 Pa and finally Mach 4 - 8 Pa. In both figures, the order of rarefaction degree is respected but there is a large difference between the Mach 2 nozzle and the two Mach 4. This observation shows that the best rarefaction parameter to describe the evolution of the shock angle is a product between the density and the Mach number.

With this last observation, two formulas were found to describe the evolution of the shock wave angle (upper and lower shock wave) as a function of the angle of attack, free stream density and Mach number. Parameter ξ is defined as $\xi = \rho_\infty (1+0.2M^2)^{2.5} M$

$$\mu = (3.8\times10^{-3}\theta + 9.1\times10^{-1})\sqrt{\frac{1}{2\xi}} + 7.72\times10^{-1}\theta + 13.2 \tag{1}$$

$$\alpha = (-1.31\times10^{-2}\theta + 1.02)\sqrt{\frac{1}{0.09\xi^{0.6}}} - 4.12\times10^{-4}\theta^3 + 3.20\times10^{-2}\theta^2 - 8.73\times10^{-1}\theta + 10.7 \tag{2}$$

These formulas are based on the experimental data. On Figure 8 and Figure 9 we plotted experimental and calculated points. It can be noted that there is good agreement between the fitting equation and the experimental data suggesting that these equations could be applied to determine the shock angles for any other flow condition.

These formulas allow to complete the study and estimate the evolution of the nozzle Mach 4 - 71 Pa shock wave angles.

4.3. Shock wave impact on aerodynamic forces

The aerodynamic forces, drag and lift, are here the consequence of the interaction between the waverider and the flow density distribution around the geometry. As presented in the previous section, the shock wave can be divided into two regions, the upper and lower shock wave. Together, they create

an equilibrium that is reflected in the aerodynamic forces. In this section, the aerodynamic forces and the shock angles are correlated by the relationship $\mu - \alpha - \theta$. As presented in the Figure 10, μ is the upper angle of the shock wave, α is the lower angle of the shock and θ is the angle of attack. When this relationship is expressed as a function of α - ω, with ω the corner angle of the waverider equal to 3.72 degrees, the Figure 11 shows that a relation between forces and shock angles can be drawn.

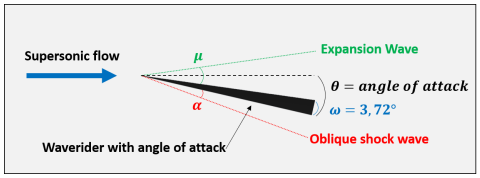

Fig. 10: Shock wave angles

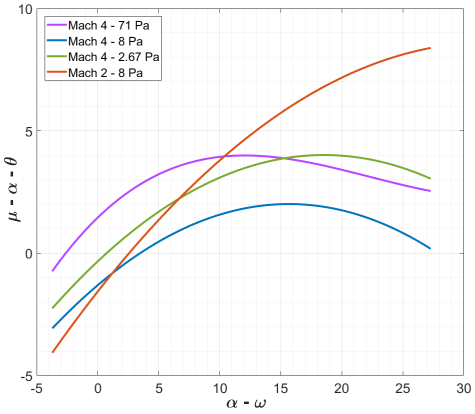

Fig. 11: Optimal angle of attack from shock wave angle analysis

For the four flow conditions studied, the shape of the curves is similar and has a maximum. When the figure is correlated with Figure 7, it can be seen that the curves have a similar shape and the maximum of the curves is located for the same angles of attack as the Lift-to-Drag ratio curves. This result highlights the link between the aerodynamic forces and the angles of attack. The Figure 11 can help to determine the optimal Lift-to-Drag ratio for any flow condition as long as shock angles are known. These values are obtained with the two equations presented earlier. Thus, when designing the waverider, it is possible to know the optimal angle of attack for any rarefied flow so at any moment of the re-entry when the velocity and density of the flow are known. This behavior can be also correlated with the pressure variation across the shock. However formulas are valid for this waverider and other studies like this one can allow to generalize formulas to all geometries.

Pitot measures could be made to obtain pressure profile at upper and lower shock angles to understand reasons of the maximum of Lift-to-Drag ratio.

5. CONCLUSION

Experimental data were obtained for aerodynamic forces and shock wave angles in slip regime in Mach 2 and 4. The model is a waverider designed by Rolim and optimized for Mach 10 and 50 km of altitude. Lift-to-Drag ratio was determined for different angle of attack ranged between 0 and 25 degrees and at several experimental condition. Results shows that the angle of attack for the best L/D value decreases when increasing Mach number and free stream pressure. The analysis of the evolution of the shock wave angles presents a strong relation with the aerodynamic behavior. This means that to improve the performances of waveriders flight at any altitude, viscous layers should be considered when designing the waverider. For this purpose, this study proposes a relation to predict shock wave angles depending on one hand on Mach number and free stream density and on the other hand on the angle of attack. Further experiments with Mach 20.2 - 6.8×10^{-2} Pa free stream pressure (100 km atmospheric altitude), will be carried out to first obtain experimental data at strong viscous flows and eventually validate the results presented in this work.

6. ACKNOWLEDGMENTS

This work is fully financed by the Agence Nationale de la Recherche for the project APHYRA (APHYRA-19-ASTR-0014-01). PhD is supported by the French National Research Agency (ANR) as part of the Programme d'Investissements d'Avenir (LabEx CAPRYSSES; Grant No ANR-11-LABX-0006-01).

7. REFERENCES

[1] Helley M Sayler, *Hypersonic weapons: Background and issues for Congress*, Congressional Research Service, 2019.

[2] John D Anderson Jr, Mark J Lewis, Ajay P Kothari, and Stephen Corda, "Hypersonic waveriders for planetary atmospheres," *Journal of Spacecraft and Rockets*, vol. 28, no. 4, pp. 401–410, 1991.

[3] J Haney, "A waverider derived hypersonic x-vehicle," in *International Aerospace Planes and Hypersonics Technologies*, p. 6162. 1995.

[4] Steven Walker, Jeffrey Sherk, Dale Shell, Ronald Schena, John Bergmann, and Jonathan Gladbach, "The darpa/af falcon program: the hypersonic technology vehicle# 2 (htv-2) flight demonstration phase," in *15th*

AIAA International Space Planes and Hypersonic Systems and Technologies Conference, 2008, p. 2539.

[5] Ki-Young Hwang and Hwanil Huh, "Research and development trends of a hypersonic glide vehicle (hgv)," *Journal of the Korean Society for Aeronautical & Space Sciences*, vol. 48, no. 9, pp. 731–743, 2020.

[6] He Linshu, Xu Dajun, et al., "Optimal trajectory analysis of hypersonic boost-glide waverider with heat load constraint," *Aircraft Engineering and Aerospace Technology: An International Journal*, 2015.

[7] Chunyun Dong, Zhi Guo, and Xiaolong Chen, "Robust trajectory planning for hypersonic glide vehicle with parametric uncertainties," *Mathematical Problems in Engineering*, vol. 2021, 2021.

[8] STI Rizvi, H Linshu, X Dajun, and SIA Shah, "Trajectory optimisation for a rocket-assisted hypersonic boost-glide vehicle," *The Aeronautical Journal*, vol. 121, no. 1238, pp. 469–487, 2017.

[9] YU Jianglong, DONG Xiwang, LI Qingdong, REN Zhang, and LV Jinhu, "Cooperative guidance strategy for multiple hypersonic gliding vehicles system," *Chinese Journal of Aeronautics*, vol. 33, no. 3, pp. 990–1005, 2020.

[10] Maurice L Rasmussen, "Waverider configurations derived from inclined circular and elliptic cones," *Journal of Spacecraft and Rockets*, vol. 17, no. 6, pp. 537–545, 1980.

[11] Paul A Chambre and Samuel A Schaaf, *Flow of rarefied gases*, Princeton University Press, 2017.

[12] John Anderson, Jr and Mark Lewis, "Hypersonic waveriders-where do we stand?," in *31st Aerospace Sciences Meeting*, 1993, p. 399.

[13] Stephen Corda and John Anderson, Jr, "Viscous optimized hypersonic waveriders designed from axisymmetric flow fields," in *26th aerospace sciences meeting*, 1988, p. 369.

[14] JD Anderson Jr, KG Bowcutt, and D Capriotti, "Viscous optimized hypersonic waveriders," AIAA-87-0272. AIAA 25th Aerospace Science Meeting, 1987.

[15] Kevin Bowcutt, "A perspective on the future of aerospace vehicle design," in *12th AIAA International Space Planes and Hypersonic Systems and Technologies*, p. 6957. 2003.

[16] D Rault, R Wilmoth, and G Bird, "An efficient dsmc algorithm applied to a delta wing," in *26th Thermophysics Conference*, 1991, p. 1316.

[17] Frederick Kautz, II and Judson Baron, "Direct simulation of waveriders in hypersonic rarefied flow," in *26th Thermophysics Conference*, 1991, p. 1317.

[18] J Allègre and C Bisch, "Angle of attack and leading edge effects on the flow about a flat plate at mach number 18.," *AIAA Journal*, vol. 6, no. 5, pp. 848–852, 1968.

[19] Jean Allegre, Didier Lartigue, and Marie-Francoise Scibilia, "Rarefied hypersonic flow characteristics of delta wings and trailing edge spoilers," *AIAA Journal*, vol. 10, no. 7, pp. 900–905, 1972.

[20] K Nagashetty, Biswajit Medhi, R Sriram, G Jagadeesh, and KPJ Reddy, "Tomographic visualization of the hypersonic flow field over a waverider," in *30th International Symposium on Shock Waves 2*. Springer, 2017, pp. 1437–1440.

[21] Tiago Cavalcanti Rolim, Paulo Gilberto de Paula Toro, Marco Antonio Sala Minucci, Antônio de Carlos de Oliveira, and Roberto da Cunha Follador, "Experimental results of a mach 10 conical-flow derived waverider to 14-x hypersonic aerospace vehicle," *Journal of Aerospace Technology and Management*, vol. 3, pp. 127–136, 2011.

[22] Charles E Cockrell Jr, Lawrence D Huebner, and Dennis B Finley, "Aerodynamic characteristics of two waverider-derived hypersonic cruise configurations," 1996.

[23] EM Galloway, MR Gilmore, RW Jeffery, and JK Harvey, "Heat transfer to a delta wing and two waverider wings in rarefied hypersonic flow," *Rarefied gas dynamics*, pp. 505–513, 1991.

[24] MN Macrossan, "Scaling parameters for hypersonic flow: correlation of sphere drag data," 2007.

[25] John Anderson, Jr, Frederick Ferguson, and Mark Lewis, "Hypersonic waveriders for high altitude applications," in *29th Aerospace Sciences Meeting*, 1991, p. 530.

[26] Jean Allègre, *Problèmes d'interactions liées aux régimes d'écoulements supersoniques et hypersoniques raréfiés*, Ph.D. thesis, 1979.

[27] Noubel Hugo and Viviana Lago, "Experimental analysis of waverider lift-to-drag ratio measurements in rarefied and supersonic regime," 2021.

[28] Eric Menier, *Influence d'une décharge électrique continue sur un écoulement supersonique raréfié*, Ph.D. thesis, Orléans, 2007.

[29] John David Anderson Jr, *Fundamentals of aerodynamics*, Tata McGraw-Hill Education, 2010.